

Ferroelectricity and piezoelectricity in soft biological tissue: Porcine aortic walls revisited

Thomas Lenz, Regina Hummel, Ilias Katsouras, Wilhelm A. Groen, Marlies Nijemeisland, Robert Ruedmler, Michael K. E. Schäfer, and Dago M. de Leeuw

Citation: *Appl. Phys. Lett.* **111**, 133701 (2017); doi: 10.1063/1.4998228

View online: <http://dx.doi.org/10.1063/1.4998228>

View Table of Contents: <http://aip.scitation.org/toc/apl/111/13>

Published by the [American Institute of Physics](#)

Articles you may be interested in

[Ferroelectric properties of lightly doped La:HfO₂ thin films grown by plasma-assisted atomic layer deposition](#)
Applied Physics Letters **111**, 132903 (2017); 10.1063/1.4999291

[Promising ferroelectricity in 2D group IV tellurides: a first-principles study](#)
Applied Physics Letters **111**, 132904 (2017); 10.1063/1.4996171

[Hybrid reflections from multiple x-ray scattering in epitaxial oxide films](#)
Applied Physics Letters **111**, 131903 (2017); 10.1063/1.4993477

[Broadband and high-efficiency circular polarizer based on planar-helix chiral metamaterials](#)
Applied Physics Letters **111**, 113503 (2017); 10.1063/1.4990142

[Multiscale identification of local tetragonal distortion in NaNbO₃-BaTiO₃ weak relaxor ferroelectrics by Raman, synchrotron x-ray diffraction, and absorption spectra](#)
Applied Physics Letters **111**, 132901 (2017); 10.1063/1.4995009

[Defect induced polarization and dielectric relaxation in Ga_{2-x}Fe_xO₃](#)
Applied Physics Letters **111**, 132902 (2017); 10.1063/1.4995570



5 Electronic Measurement Pitfalls to Avoid

Get the whitepaper

Ferroelectricity and piezoelectricity in soft biological tissue: Porcine aortic walls revisited

Thomas Lenz,^{1,2,a)} Regina Hummel,³ Ilias Katsouras,⁴ Wilhelm A. Groen,^{4,5} Marlies Nijemeisland,⁵ Robert Ruemmler,³ Michael K. E. Schäfer,^{3,6} and Dago M. de Leeuw^{1,5}

¹Max Planck Institute for Polymer Research, Ackermannweg 10, 55128 Mainz, Germany

²Graduate School Materials Science in Mainz, Staudinger Weg 9, 55128 Mainz, Germany

³Department of Anesthesiology, University Medical Center, Johannes Gutenberg-University Mainz, Langenbeckstr. 1, 55131 Mainz, Germany

⁴Holst Centre, High Tech Campus 31, 5656AE Eindhoven, The Netherlands

⁵Faculty of Aerospace Engineering, Delft University of Technology, Kluyverweg 1, 2629 HS Delft, The Netherlands

⁶Focus Program Translational Neurosciences (FTN), University Medical Center, Johannes Gutenberg-University Mainz, Langenbeckstr. 1, 55131 Mainz, Germany

(Received 29 July 2017; accepted 12 September 2017; published online 29 September 2017)

Recently reported piezoresponse force microscopy (PFM) measurements have proposed that porcine aortic walls are ferroelectric. This finding may have great implications for understanding biophysical properties of cardiovascular diseases such as arteriosclerosis. However, the complex anatomical structure of the aortic wall with different extracellular matrices appears unlikely to be ferroelectric. The reason is that a prerequisite for ferroelectricity, which is the spontaneous switching of the polarization, is a polar crystal structure of the material. Although the PFM measurements were performed locally, the phase-voltage hysteresis loops could be reproduced at different positions on the tissue, suggesting that the whole aorta is ferroelectric. To corroborate this hypothesis, we analyzed entire pieces of porcine aorta globally, both with electrical and electromechanical measurements. We show that there is no hysteresis in the electric displacement as well as in the longitudinal strain as a function of applied electric field and that the strain depends on the electric field squared. By using the experimentally determined quasi-static permittivity and Young's modulus of the fixated aorta, we show that the strain can quantitatively be explained by Maxwell stress and electrostriction, meaning that the aortic wall is neither piezoelectric nor ferroelectric, but behaves as a regular dielectric material. *Published by AIP Publishing.*

[<http://dx.doi.org/10.1063/1.4998228>]

Piezoelectricity in bones was first reported in 1957.¹ The main components of bone are the mineral hydroxyapatite $\text{Ca}_{10}(\text{PO}_4)_6(\text{OH})_2$ and collagen.² The unit cell of hydroxyapatite, P63/m, is centrosymmetric and, therefore, this natural mineral cannot be piezoelectric.³ We note that polymorphs with non-centrosymmetric unit cells have been predicted.⁴ Recently, piezoelectricity was confirmed in synthetic hydroxyapatite, namely, in electrically poled, textured ceramics⁵ and in nanocrystalline thin films.⁶ In short, the piezoelectricity in bones is due to collagen. The polypeptide chains in collagen are arranged in a coiled-coil triple helix forming rod-like molecules with short-range crystallinity.⁷ The quasi-hexagonal packing of oriented collagen molecules, with symmetry group C_6 ,⁸ leads to shear piezoelectricity in the axial direction; dry bone polarizes when a shearing force acts on the oriented collagen fibers so that they slip past one another. The piezoelectric charge coefficient, d_{14} , for dry horse femur⁸ and dry bovine⁹ bone is in the order of 0.2 pC/N. Other constants, such as d_{33} in the longitudinal direction, are negligible.¹⁰

Both the direct and the converse piezoelectric effect have been demonstrated. The extracted linear relationship between electrical displacement and stress, as well as between electric field and strain, proves that bones are truly piezoelectric,¹ as

they demonstrate interconversion between electrical charge and mechanical strain. The electromechanical coupling of oriented collagen fibers can have significant consequences for human physiology.¹¹ For instance, it might explain Wolff's law, stating that bone in a healthy person or animal remodels itself under an applied mechanical load.^{12–14} We note also that, recently, piezoelectricity has been suggested as a toughening mechanism in seashells.¹⁵

Piezoelectricity has been reported not only in calcified biological tissue, such as bone and teeth, but also in soft biological tissues such as ligament, trachea, and intestines.¹⁶ The electromechanical coupling is not limited to collagen, but observed in a variety of biopolymers such as cellulose, elastin, keratin,¹⁷ and chitin, which suggests that all fibrous molecules in an oriented state are piezoelectric.

By definition, polycrystalline materials with randomly oriented grains must be ferroelectric in order to exhibit piezoelectric properties.¹⁸ Ferroelectricity means that the material exhibits a spontaneous polarization, which can be switched by an electric field.¹⁹ However, despite the “near-ubiquitous presence of piezoelectricity in biological systems,”²⁰ there has been very limited evidence for ferroelectricity, especially in soft tissues. The first reports of a ferroelectric response in porcine aortic walls by means of piezoresponse force microscopy (PFM)^{21–24} were therefore surprising. PFM detects the

^{a)}E-mail: lenz@mpip-mainz.mpg.de

local deformation of a sample caused by an applied electric field from the tip of the cantilever of a scanning force microscope.^{25,26} For the porcine aorta, the reversal in the piezoresponse phase occurred at about 10 V leading to an estimated coercive field of only 10 kV/m,²¹ three orders of magnitude smaller than typical ferroelectric polymers such as polyvinylidene difluoride (PVDF).²⁷ It was argued that the asymmetry in the coercive voltage could reflect the existence of an internal polarization, as the aorta is internally biased outward.²⁸ The phase contrast was approximately 180°, which is a clear indication of polarization switching. Associated with the phase reversal, the deformation-voltage butterfly loops were also observed. The piezoelectric charge coefficient was estimated to be 1 pm/V.²¹ It was noted that this value is two orders of magnitude larger than the one previously reported for blood vessel walls, measured on a macroscopic scale.¹⁶ Although the PFM measurements were performed locally, the phase-voltage hysteresis loops obtained at different points of the sample were consistent, which indicated global ferroelectricity of the whole aortic tissue.

The ferroelectricity was claimed to be due to the presence of elastin,²² an important extracellular matrix protein found in connective tissue. The fibrillar component of elastin consists of simple amino acids such as glycine, valine and alanine.²⁹ Both crystalline γ -glycine^{30,31} and β -glycine³² are ferroelectric, yet the aorta is not a single crystal. Hence, the reported PFM switching in both aortic walls and elastin was unexpected, and has generated a lot of excitement, but considerable skepticism remains. The latter was expressed, for instance, in the following statement: “Readers should keep in mind that crystalline ferroelectrics are not known to exist in humans, and no *in vitro* or even *in situ* work has been reported.”³³ Here, we contribute to the scientific discussion on biological ferroelectricity by analyzing porcine aorta globally instead of only locally. To that end, we measured both electric displacement and strain as a function of applied electric field on a 1 cm² piece of porcine aorta. We observed neither ferroelectric nor piezoelectric response of the fixated tissue. The strain is proportional to the electric field squared, which indicates that the strain is due to both Maxwell stress and electrostriction, phenomena that occur in any dielectric material.

The aorta specimens were prepared following a procedure reported in the Supporting Information of Ref. 21. In short, about 12 cm of aortas (middle section) was harvested from pigs (*sus scrofa domestica*), which were part of an experimental lung physiology study at the University Medical Center of Mainz. After removal of surrounding fat and tissue, the aortas were immediately immersed in ice-cold phosphate-buffered saline (PBS). The tissue was always kept at 4 °C until final fixation. Figure 1(a) shows a photograph of a piece of the descending thoracic aorta.

For histology, cleaned aortic samples were snap frozen and sectioned into 10 μ m slices with a cryostat (HM 560 Cryo-Stat, Thermo Scientific). In order to illustrate cells and elastic fibers, a van Gieson stain was applied. Histological images were acquired using a conventional light microscope (AxioVert200, Zeiss) at 10 \times and 40 \times magnification and are shown in Fig. 1(b). The general structure of blood vessels can be subdivided into the intima, media, and adventitia

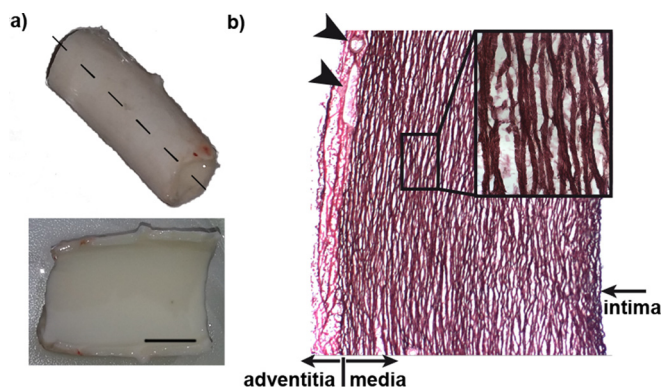


FIG. 1. (a) Photograph of the descending thoracic aorta before fixation. Upper picture shows the circular aorta, while the lower picture demonstrates tissue sample cut open at the dotted line with the inner wall (intima) on top. Scale bar is 1 cm. (b) Histological image of the aorta illustrating the cross-section of the aortic wall (adventitia, media, and intima, 10 \times). The inset shows a 40 \times magnification of elastic fibers in the media. Arrowheads point to small vessels inside the adventitia.

from the inside out.^{34–37} The intima with its endothelial cells delimits the vessel wall from the lumen. The media with smooth muscle cells and connective tissue such as elastin fibers [see inset of Fig. 1(b)] accounts for the majority of the vascular wall, especially in big arteries. The adventitia represents the border to the tissue surrounding the vessel, frequently with its own blood supply.

For electrical and mechanical characterization, porcine aortic samples with an area of about 1 cm² and a thickness of 1 mm were fixated using 4% paraformaldehyde in PBS for 1 h at ambient temperature. Then, samples were dehydrated in an ascending ethanol/deionized water series for 15 min each (30/70; 50/50; 70/30; 100/0). Afterwards samples were subjected to an ascending hexamethyldisilazane/ethanol series (30/70; 50/50; 70/30; 100/0) for 15 min each and finally dried overnight in a hood.

Uniaxial tensile tests were performed on an Instron Model 3365 universal testing system equipped with a 1 kN load cell. Tensile specimens of fixated porcine aorta, having an approximate width of 5 mm, a thickness of 1 mm and a length of 4 mm, were stretched between the clamps with a tensile rate of 1 mm/min at ambient temperature.

The electric displacement as a function of electric field was measured using a Radiant precision multiferroic test system (Radiant Technologies, Inc.) at a frequency of 10 Hz. Simultaneously, the strain as a function of electric field was measured using a MTI 2100 photonic sensor interfaced with the Radiant tester. Piezoelectricity was additionally investigated using a Berlincourt-type piezometer (PM300, Piezotest, London, UK). A static force of 10 N was used under a 0.25 N peak to peak sinusoidal excitation at 110 Hz. Impedance was measured using a Schlumberger Si 1260 Impedance Analyzer. All electrical measurements were performed in ambient conditions. We emphasize that we tested aortas from two different pigs and various pieces from each aorta. Our results could be reproduced in all the tests.

Figure 2(a) shows the electric displacement versus electric field. Electrical conduction can be excluded as the dielectric loss is less than 1%. A linear relation is obtained up to the maximum electric field of about 6 MV/m, which is

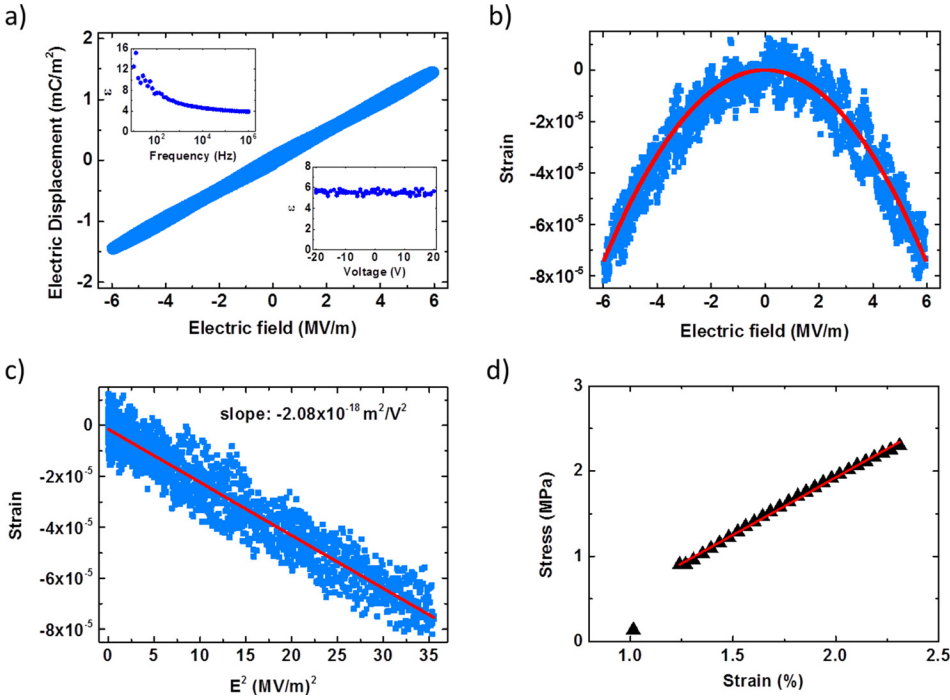


FIG. 2. Electro-mechanical characterization of aortic walls. (a) Electrical displacement as a function of electric field. The top inset shows the dispersion in relative dielectric constant. The bottom inset shows the relative dielectric constant as a function of voltage measured at 1 kHz. (b) Strain as a function of electric field. (c) Strain as a function of electric field squared. (d) Stress-strain curve. From the slope between 1% and 2% the Young's modulus is obtained as 160 ± 20 MPa.

much larger than the coercive field of 10 kV/m extracted from reported PFM measurements. However, there is no indication of hysteresis as would have been expected for a ferroelectric capacitor. The aortic specimen behaves as a normal dielectric. The bottom inset shows that the relative dielectric constant at 1 kHz is about 6 and independent of the applied bias. The top inset shows the frequency dependence. The dispersion could be due to ionic movement or minute amounts of residual water. We take a value of 26 for the quasi-static relative dielectric constant as extracted from the slope of the displacement as a function of electric field, cf. Fig. 2(a).

The electrical displacement, D , for a capacitor under an applied electric field, E , is the sum of the induced polarization, P_i , and spontaneous polarization P_s ³⁸

$$D = P_i + P_s = \epsilon_0 \epsilon_r E + P_s = \epsilon_0 \epsilon_r E, \quad (1)$$

where ϵ_0 is the vacuum permittivity and ϵ_r is the relative dielectric constant. The spontaneous polarization is due to aligned electric dipoles in a ferroelectric material and depends on the electric field and the poling history. However, this non-linear contribution to the displacement can be disregarded for the aorta, $P_s = 0$, as there is no hysteresis in the displacement as function of electric field, cf. Fig. 2(a). There is no sign of a ferroelectric spontaneous polarization. The displacement is only due to the induced polarization, which represents the charging of any linear dielectric capacitor.

To investigate the electromechanical properties of the porcine aortic wall, we measured the strain as a function of electric field, as presented in Fig. 2(b). The strain is negative; the aorta specimen contracts when an electric field is applied. Here again, there is no indication of hysteresis; a butterfly shape as expected for ferroelectric materials is not observed. The shape of the strain versus electrical displacement curve looks like a parabola. As verification we present the strain as a function of electric field squared in Fig. 2(c). A straight line is indeed obtained and the least square approximation

yields a slope of $-2.08 \times 10^{-18} \text{ m}^2/\text{V}^2$. This value also allows fitting the measured data in Fig. 2(b), as indicated by the red lines.

The aortic wall is hence not ferroelectric, but also not piezoelectric as additionally supported by Berlincourt-type piezometer measurements. No measurable signal could be detected for d_{33} , d_{13} , and d_{15} demonstrating that the aortic wall is not piezoelectric, i.e., there is no surface charge generated under mechanical stress.

The strain induced in a non-piezoelectric, isotropic dielectric material by an electrostatic field has two sources.³⁹ The first one is the Maxwell strain, which is due to the electrostatic force resulting from the free charges on the electrodes of a capacitor. The second one, referred to as electrostriction, is a universal property of solid and liquid dielectrics^{40,41} arising from changes in the dielectric constant with the electrically induced strain.^{42,43} The total longitudinal strain, S_{33} , is given by^{39,42,43}

$$S_{33} = -\frac{1}{2} \epsilon_r \epsilon_0 E^2 / Y \times \left((1 + 2\nu) - \frac{-a_1 + a_2(1 - 2\nu)}{\epsilon_r} \right), \quad (2)$$

where Y is the Young's modulus, ν is the Poisson ratio, and a_1 and a_2 are two electrostrictive parameters describing the change in dielectric properties of the material under shear and bulk deformation, respectively. This equation holds for non-compliant electrodes; for compliant electrodes, the longitudinal strain is twice as large.⁴⁴ When the dielectric constant is independent of deformation, then a_1 and a_2 vanish and only the compressive Maxwell strain remains, given by the first term of Eq. (2) as

$$S_{33, \text{Maxwell}} = -\frac{1}{2} \epsilon_r \epsilon_0 E^2 / Y \times (1 + 2\nu), \quad (3)$$

and the pure electrostrictive contribution is given by the second term of Eq. (2) as

$$S_{33, \text{Electrostriction}} = \frac{1}{2} \epsilon_r \epsilon_0 E^2 / Y \times \left(\frac{-a_1 + a_2(1 - 2\nu)}{\epsilon_r} \right) = Q_{33} D^2, \quad (4)$$

where Q_{33} is the commonly used longitudinal electrostrictive coefficient, derived from the phenomenological Devonshire theory.⁴⁰ For ionic insulators, the electrostrictive strain is dominated by anharmonicity in the electrostatic potential leading to a positive Q_{33} .⁴¹ For polymers, covalent bonding is much stronger than intermolecular forces such as van der Waals interactions. This effectively leads to a negative value of Q_{33} , and, hence, to a compressive strain. Both the Maxwell- and electrostrictive strain depend on the squared electric field and are therefore indistinguishable.

In order to quantitatively analyze the strain, a value for the Young's modulus is required. Since the porcine aorta samples underwent fixation before electrical characterization, we cannot use literature values reported for fresh aortas. Therefore, we performed a tensile test for a piece of fixated porcine aorta. A typical stress-strain curve in the linear regime is presented in Fig. 2(d). From the slope between 1.0% and 2.0% strain, we extract an average Young's modulus of 160 ± 20 MPa. The process of fixation increases the stiffness of the aorta piece by two orders of magnitude with respect to a fresh porcine aorta due to denaturation of the proteins by alcohol and cross-linking by paraformaldehyde.

We calculate from Eq. (3) the Maxwell strain by taking the extracted value of 26 for the static dielectric constant, and a Poisson ratio of 0.3.⁴⁵ We calculate for the proportionality constant between strain and electric field squared a value of $-1.1 \times 10^{-18} \text{ m}^2/\text{V}^2$. This value is about half of the experimentally determined slope, cf. Fig. 2(c), meaning that about half of the strain is due to Maxwell stress. The other half of the strain is due to electrostriction, leading to an extracted electrostrictive coefficient, Q_{33} , of $-17.4 \text{ m}^4/\text{C}^2$. We note that this coefficient can be estimated from the empirical linear relation for the absolute value of the hydrostatic electrostrictive constant $Q_h = 1/\epsilon_0 \epsilon_r Y$.^{40,46} A theoretical derivation for electrostrictive polymers is reported based on a microscopic Debye/Langevin formalism.⁴⁷ The calculated value of $27 \text{ m}^4/\text{C}^2$ is in fair agreement with the experimentally extracted value for the aortic wall.

Our measurements at electric fields up to 6 MV/m allowed us to demonstrate that the strain as a function of electric field is a parabola, i.e., the strain depends on the electric field squared. In contrast, reported PFM measurements were performed at much lower fields up to only 0.1 MV/m. To compare the local and global datasets, we approximated our global strain/electric field curve as a straight line. At low fields, we then obtain a slope of 2 pm/V, which could explain the value of 1 pm/V as extracted from the reported local PFM measurements.

Our global strain measurements on aortic walls are at variance with reported PFM measurements.^{21–24} Piezoresponse force microscopy is a powerful tool and well-established in the ferroelectric community.^{25,26,48–51} However, it was demonstrated to be prone to artifacts.^{52–54} We deliberately tried, but failed to reproduce the PFM phase switching. The reported switching might be due to voltage gated ion channels

or reorientation of dipoles, which are “internally biased outward” in the aorta. These responses are not ferroelectric but remain intriguing and open for further investigation.

We gratefully acknowledge technical support from C. Bauer, H. Raich, and F. Keller, and stimulating discussions with P. W. M. Blom, all from the Max Planck Institute for Polymer Research, Mainz, Germany. We want to thank C. Möllmann from the University Medical Center for help with the extraction of the aorta. T.L. acknowledges financial support by the Graduate School Materials Science in Mainz.

- ¹E. Fukada and I. Yasuda, “On the piezoelectric effect of bone,” *J. Phys. Soc. Jpn.* **12**(10), 1158–1162 (1957).
- ²M.-J. Majid and Y. Min-Feng, “Nanoscale characterization of isolated individual type I collagen fibrils: Polarization and piezoelectricity,” *Nanotechnology* **20**(8), 085706 (2009).
- ³C. Halperin, S. Mutchnik, A. Agronin, M. Molotskii, P. Urenski, M. Salai, and G. Rosenman, “Piezoelectric effect in human bones studied in nanometer scale,” *Nano Lett.* **4**(7), 1253–1256 (2004).
- ⁴D. Haverty, S. A. M. Tofail, K. T. Stanton, and J. B. McMonagle, “Structure and stability of hydroxyapatite: Density functional calculation and Rietveld analysis,” *Phys. Rev. B* **71**(9), 094103 (2005).
- ⁵A. A. Gandhi, M. Wojtas, S. B. Lang, A. L. Kholkin, and S. A. M. Tofail, “Piezoelectricity in poled hydroxyapatite ceramics,” *J. Am. Ceram. Soc.* **97**(9), 2867–2872 (2014).
- ⁶S. B. Lang, S. A. M. Tofail, A. L. Kholkin, M. Wojtaś, M. Gregor, A. A. Gandhi, Y. Wang, S. Bauer, M. Krause, and A. Plecenik, “Ferroelectric polarization in nanocrystalline hydroxyapatite thin films on silicon,” *Sci. Rep.* **3**, 2215 (2013).
- ⁷M. D. Shoulders and R. T. Raines, “Collagen structure and stability,” *Annu. Rev. Biochem.* **78**(1), 929–958 (2009).
- ⁸E. Fukada, “Mechanical deformation and electrical polarization in biological substances,” *Biorheology* **5**(3), 199–208 (1968).
- ⁹A. R. Liboff and M. Furst, “Pyroelectric effect in collagen structures,” *Ann. N. Y. Acad. Sci.* **238**(1), 26–35 (1974).
- ¹⁰A. A. Gundjian and H. L. Chen, “Standardization and interpretation of the electromechanical properties of bone,” *IEEE Trans. Biomed. Eng.* **21**(3), 177–182 (1974).
- ¹¹C. A. L. Bassett, “Biologic significance of piezoelectricity,” *Calcif. Tissue Res.* **1**(1), 252–272 (1967).
- ¹²J. Wolff, “Ueber die innere Architectur der Knochen und ihre Bedeutung für die Frage vom Knochenwachstum,” *Arch. Pathol. Anat. Physiol. Klin. Med.* **50**(3), 389–450 (1870).
- ¹³R. Brand and L. Claes, “The law of bone remodelling,” *J. Biomech.* **22**(2), 185–187 (1989).
- ¹⁴C. A. L. Bassett, R. J. Pawluk, and R. O. Becker, “Effects of electric currents on bone *in vivo*,” *Nature* **204**(4959), 652–654 (1964).
- ¹⁵T. Li and K. Zeng, “Piezoelectric properties and surface potential of green abalone shell studied by scanning probe microscopy techniques,” *Acta Mater.* **59**(9), 3667–3679 (2011).
- ¹⁶E. Fukada and K. Hara, “Piezoelectric effect in blood vessel walls,” *J. Phys. Soc. Jpn.* **26**(3), 777–780 (1969).
- ¹⁷A. J. P. Martin, “Tribo-electricity in wool and hair,” *Proc. Phys. Soc.* **53**(2), 186 (1941).
- ¹⁸T. Ikeda, *Fundamentals of Piezoelectricity* (Oxford University Press, 1990).
- ¹⁹D. Damjanovic, “Ferroelectric, dielectric and piezoelectric properties of ferroelectric thin films and ceramics,” *Rep. Prog. Phys.* **61**(11), 1267–1324 (1998).
- ²⁰B. J. Rodriguez, S. V. Kalinin, J. Shin, S. Jesse, V. Grichko, T. Thundat, A. P. Baddorf, and A. Gruverman, “Electromechanical imaging of biomaterials by scanning probe microscopy,” *J. Struct. Biol.* **153**(2), 151–159 (2006).
- ²¹Y. Liu, Y. Zhang, M.-J. Chow, Q. N. Chen, and J. Li, “Biological ferroelectricity uncovered in aortic walls by piezoresponse force microscopy,” *Phys. Rev. Lett.* **108**(7), 078103 (2012).
- ²²Y. Liu, H.-L. Cai, M. Zelisko, Y. Wang, J. Sun, F. Yan, F. Ma, P. Wang, Q. N. Chen, H. Zheng, X. Meng, P. Sharma, Y. Zhang, and J. Li, “Ferroelectric switching of elastin,” *Proc. Natl. Acad. Sci. U.S.A.* **111**(27), E2780–E2786 (2014).

- ²³Y. Liu, Y. Wang, M.-J. Chow, N. Q. Chen, F. Ma, Y. Zhang, and J. Li, "Glucose suppresses biological ferroelectricity in aortic elastin," *Phys. Rev. Lett.* **110**(16), 168101 (2013).
- ²⁴X. Y. Liu, F. Yan, L. L. Niu, Q. N. Chen, H. R. Zheng, and J. Y. Li, "Strong correlation between early stage atherosclerosis and electromechanical coupling of aorta," *Nanoscale* **8**(13), 6975–6980 (2016).
- ²⁵E. Soergel, "Piezoresponse force microscopy (PFM)," *J. Phys. D: Appl. Phys.* **44**(46), 464003 (2011).
- ²⁶A. Gruverman and S. V. Kalinin, "Piezoresponse force microscopy and recent advances in nanoscale studies of ferroelectrics," *J. Mater. Sci.* **41**(1), 107–116 (2006).
- ²⁷M. Li, H. J. Wondergem, M.-J. Spijkman, K. Asadi, I. Katsouras, P. W. M. Blom, and D. M. de Leeuw, "Revisiting the δ -phase of poly(vinylidene fluoride) for solution-processed ferroelectric thin films," *Nat. Mater.* **12**(5), 433–438 (2013).
- ²⁸P. Boldrini, "Ferroelectricity in the arterial wall: A new physical component of atherosclerosis," *J. Theor. Biol.* **87**(2), 263–273 (1980).
- ²⁹W. F. Daamen, J. H. Veerkamp, J. C. van Hest, and T. H. van Kuppevelt, "Elastin as a biomaterial for tissue engineering," *Biomaterials* **28**(30), 4378–4398 (2007).
- ³⁰A. Heredia, V. Meunier, I. K. Bdikin, J. Gracio, N. Balke, S. Jesse, A. Tselev, P. K. Agarwal, B. G. Sumpter, S. V. Kalinin, and A. L. Kholkin, "Nanoscale ferroelectricity in crystalline γ -Glycine," *Adv. Funct. Mater.* **22**(14), 2996–3003 (2012).
- ³¹E. Seyedhosseini, I. Bdikin, M. Ivanov, D. Vasileva, A. Kudryavtsev, B. J. Rodriguez, and A. L. Kholkin, "Tip-induced domain structures and polarization switching in ferroelectric amino acid glycine," *J. Appl. Phys.* **118**(7), 072008 (2015).
- ³²E. Seyedhosseini, K. Romanyuk, D. Vasileva, S. Vasilev, A. Nuraeva, P. Zelenovskiy, M. Ivanov, A. N. Morozovska, V. Y. Shur, H. Lu, A. Gruverman, and A. L. Kholkin, "Self-assembly of organic ferroelectrics by evaporative dewetting: A case of β -Glycine," *ACS Appl. Mater. Interfaces* **9**(23), 20029–20037 (2017).
- ³³J. F. Scott, "Prospects for Ferroelectrics: 2012–2022," *ISRN Mater. Sci.* **2013**, 24.
- ³⁴A. Tsamis, J. T. Krawiec, and D. A. Vorp, "Elastin and collagen fibre microstructure of the human aorta in ageing and disease: A review," *J. R. Soc. Interface* **10**(83), 20121005 (2013).
- ³⁵Z. Tonar, T. Kubíková, C. Prior, E. Demjén, V. Liška, M. Králíčková, and K. Witter, "Segmental and age differences in the elastin network, collagen, and smooth muscle phenotype in the tunica media of the porcine aorta," *Ann. Anat.* **201**, 79–90 (2015).
- ³⁶P. W. Alford, J. D. Humphrey, and L. A. Taber, "Growth and remodeling in a thick-walled artery model: Effects of spatial variations in wall constituents," *Biomech. Model. Mechanobiol.* **7**(4), 245–262 (2008).
- ³⁷A. M. Robertson and P. N. Watton, "Mechanobiology of the arterial wall," in *Transport in Biological Media* (Elsevier, 2013), pp 275–347.
- ³⁸I. Katsouras, K. Asadi, M. Li, T. B. van Driel, K. S. Kjaer, D. Zhao, T. Lenz, Y. Gu, P. W. M. Blom, D. Damjanovic, M. M. Nielsen, and D. M. de Leeuw, "The negative piezoelectric effect of the ferroelectric polymer poly(vinylidene fluoride)," *Nat. Mater.* **15**(1), 78–84 (2016).
- ³⁹I. Krakovský, T. Romijn, and A. Posthuma De Boer, "A few remarks on the electrostriction of elastomers," *J. Appl. Phys.* **85**(1), 628–629 (1999).
- ⁴⁰R. E. Newnham, V. Sundar, R. Yimnirun, J. Su, and Q. M. Zhang, "Electrostriction: Nonlinear electromechanical coupling in solid dielectrics," *J. Phys. Chem. B* **101**(48), 10141–10150 (1997).
- ⁴¹F. Li, L. Jin, Z. Xu, and S. Zhang, "Electrostrictive effect in ferroelectrics: An alternative approach to improve piezoelectricity," *Appl. Phys. Rev.* **1**(1), 011103 (2014).
- ⁴²O. P. Thakur and N. Agrawal, "Modelling of sensing performance of electrostrictive capacitive sensors," in *Sensing Technology: Current Status and Future Trends III*, edited by A. Mason, S. C. Mukhopadhyay, and K. P. Jayasundera (Springer International Publishing, Cham, 2015), pp. 341–358.
- ⁴³O. P. Thakur and A. K. Singh, "Electrostriction and electromechanical coupling in elastic dielectrics at nanometric interfaces," *Mater. Sci. - Poland* **27**(3), 839–850 (2009).
- ⁴⁴R. E. Pelrine, R. D. Kornbluh, and J. P. Joseph, "Electrostriction of polymer dielectrics with compliant electrodes as a means of actuation," *Sens. Actuators, A* **64**(1), 77–85 (1998).
- ⁴⁵G. N. Greaves, A. L. Greer, R. S. Lakes, and T. Rouxel, "Poisson's ratio and modern materials," *Nat. Mater.* **10**(11), 823–837 (2011).
- ⁴⁶R. Yimnirun, S. Eury, V. Sundar, P. J. Moses, and R. E. Newnham, "Compressometer based method for measuring converse electrostriction in polymers," in *Conference on Electrical Insulation and Dielectric Phenomena (CEIDP), Annual Report* (1999), pp. 338–341.
- ⁴⁷J. F. Capsal, M. Lallart, J. Galineau, P. J. Cottinet, G. Sebald, and D. Guyomar, "Evaluation of macroscopic polarization and actuation abilities of electrostrictive dipolar polymers using the microscopic Debye/Langevin formalism," *J. Phys. D: Appl. Phys.* **45**(20), 205401 (2012).
- ⁴⁸D. Denning, J. Guyonnet, and B. J. Rodriguez, "Applications of piezoresponse force microscopy in materials research: From inorganic ferroelectrics to biopiezoelectrics and beyond," *Int. Mater. Rev.* **61**(1), 46–70 (2016).
- ⁴⁹D. A. Bonnell, S. V. Kalinin, A. L. Kholkin, and A. Gruverman, "Piezoresponse force microscopy: A window into electromechanical behavior at the nanoscale," *MRS Bull.* **34**(9), 648–657 (2009).
- ⁵⁰S. Jesse, A. P. Baddorf, and S. V. Kalinin, "Switching spectroscopy piezoresponse force microscopy of ferroelectric materials," *Appl. Phys. Lett.* **88**(6), 062908 (2006).
- ⁵¹S. V. Kalinin, B. J. Rodriguez, S. Jesse, T. Thundat, and A. Gruverman, "Electromechanical imaging of biological systems with sub-10 nm resolution," *Appl. Phys. Lett.* **87**(5), 053901 (2005).
- ⁵²B. Kim, D. Seol, S. Lee, H. N. Lee, and Y. Kim, "Ferroelectric-like hysteresis loop originated from non-ferroelectric effects," *Appl. Phys. Lett.* **109**(10), 102901 (2016).
- ⁵³J. S. Sekhon, L. Aggarwal, and G. Sheet, "Voltage induced local hysteretic phase switching in silicon," *Appl. Phys. Lett.* **104**(16), 162908 (2014).
- ⁵⁴N. Balke, P. Maksymovych, S. Jesse, A. Herklotz, A. Tselev, C.-B. Eom, I. I. Kravchenko, P. Yu, and S. V. Kalinin, "Differentiating ferroelectric and nonferroelectric electromechanical effects with scanning probe microscopy," *ACS Nano* **9**(6), 6484–6492 (2015).